Sink Flow Deforms the Interface Between a Viscous Liquid and Air into a Tip Singularity

S. Courrech du Pont and J. Eggers
School of Mathematics, University of Bristol, University Walk, Bristol BS8 1TW, United Kingdom
(Received 9 September 2005; published 23 January 2006)

In our experiment, an interface between a viscous liquid and air is deformed by a sink flow of constant flow rate to form a sharp tip. Using a microscope, the interface shape is recorded down to a tip size of 1 μm. The curvature at the tip is controlled by the distance h between the tip and the sink. As a critical distance h^* is approached, the curvature diverges like $1/(h-h^*)^3$ and the tip becomes cone shaped. As the distance to the sink is decreased further, the opening angle of the cone vanishes like h^2. No evidence for air entrainment was found, except when the tip was inside the orifice.

DOI: 10.1103/PhysRevLett.96.034501 PACS numbers: 47.20.Ma, 47.15.G−, 47.55.D−

Hydrodynamics very often leads to the spontaneous formation of very small structures, such as in the separation of a liquid drop from a nozzle [1,2], drop coalescence [3], shock waves [4], free-surface cusps [5,6], or tips [7–9]. Mathematically, all the above phenomena correspond to a singularity [10,11] of an underlying hydrodynamic equation, in which the hydrodynamic fields become nonsmooth. Hydrodynamic singularities can be classified into two groups. In the first group of ''true'' singularities the production of small scales is cut off only by a microscopic length, such as the size of a molecule. In the second group, there exists some hydrodynamic mechanism which is able to ''regularize'' the singularity. In the past, all singularities which persist for a finite amount of time were found to belong to the second group, typical regularizing mechanisms being diffusion [4], surface tension [12], or the presence of an outer liquid [6]. By contrast, in this Letter we describe a stationary tip whose typical size is not limited by any hydrodynamic mechanism, such as surface tension.

Tips were first investigated by G. I. Taylor [7], by placing a liquid drop of small viscosity in a viscous flow produced by counter-rotating rollers, stretching the drop. At its ends, the drop develops tips which become quite sharp, yet it has never been established whether the tip remains rounded on some scale [13]. Tips have recently received intense scrutiny [8,14,15] owing to their potential in producing extremely thin jets, leading to numerous microfluidic applications [14,16,17]. In the viscous withdrawal experiment [8,15] a liquid is withdrawn through a straw placed above a liquid-liquid interface, producing a sharp ''hump''. While the curvature of the hump appears to diverge as the flow rate is increased, the (apparent) singularity is actually cut off at a typical size of 0.2 mm [15], and the hump transforms into a jet.

In the present experiment we replace one of the liquids by a gas, finding no sign of the disappearance of the tip. Hence we are able to track the approach to the singularity (i.e., a divergence of the tip curvature) over 4 orders of magnitude, the curvature being described by a universal scaling law. Three-dimensional axisymmetric flow thus appears to be fundamentally different from a two-dimensional one [12], in that surface tension does not succeed in regularizing the tip singularity. The presence of a singularity also raises exciting prospects to produce structures by hydrodynamic forcing whose size is only limited by microscopic features [18].

Our experimental setup, sketched in Fig. 1, consists of a $27 \times 27 \times 130$ mm cell partially filled with a viscous liquid (we used castor oil and two different silicone oils). The liquid flows out of a hole ($a = 1$ and 3 mm in diameter) drilled into a circular plate of 0.7 mm thickness. The flow rate $Q \equiv Q_{\text{out}}$ is adjusted to a constant value by the ball valve (1), and measured by weighing. To ensure stationary conditions, the flow rate Q_{in} into the cell is adjusted by the valve (2) to be almost equal but smaller than Q_{out}. In the course of a typical experiment, the cell empties over a period of 2–6 hours at constant Q, thus adiabatically changing the filling height H of the container.

All results reported here are for stationary and low Reynolds number flow. It thus differs from [9], which contains a significant time dependence. The interface shape (cf. Fig. 2) is recorded using a microscope with a working distance of 20 mm and a high resolution CCD

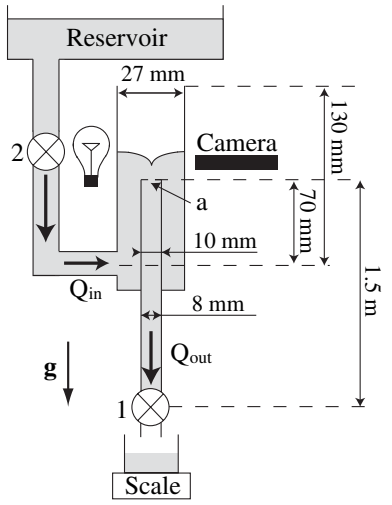

FIG. 1. Sketch of the experimental setup.

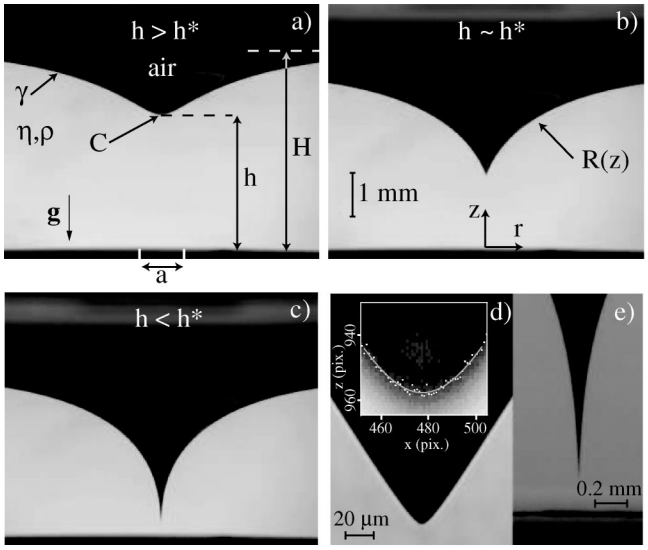

FIG. 2. Photographs of the air-liquid interface (silicone oil, $\eta = 60$ Pa s and $Q = 3.9 \times 10^{-3}$ ml s^{-1}). (a) $h > h^*$, (b) $h = h^*$, (c) $h < h^*$. (d) A Gaussian fit to the tip just before the singularity. (e) the tip as it is about to enter the orifice.

camera. The overall resolution of the optics is 1 μm. The benefit of using gravity to drive the flow is that no unsteadiness could be detected down to a micron scale, but we are limited in the achievable flow rates. Our attempts of using a pump for driving failed owing to unsteadiness of the interface caused by mechanical vibrations.

Backlighting ensures a sharp gray-level gradient at the interface, and profiles $R(z)$ were extracted in numerical form using image processing software. Axisymmetry is preserved to within our experimental resolution. First we focus on the development of a sharp tip, shown in Figs. 2(a) and 2(b). To that end we determine the curvature C at the tip, by fitting a Gaussian and a parabolic profile [cf. Fig. 2(d)] to it. Figure 3 shows the curvature as a function of the distance h from the orifice to the tip for various flow rates Q, using the same silicone oil of viscosity $\eta = 30$ Pa s, surface tension $\gamma = 2.13 \times 10^{-2}$ Nm^{-1}, and density $\rho = 976$ kg/m^3. As h reaches a *critical* value h^*, the curvature diverges like $1/(h - h^*)^3$, as shown in the inset for one data set. The same exponent -3 ± 0.2 is observed for all our data sets. Albeit for a limited range, the data of [9] for H is also consistent with ours.

We now show that the singularity occurs when the tip experiences a critical viscous forcing, relative to the smoothing effects of surface tension. Namely, in the limit of slow flow a point sink in a solid plate produces a velocity $3Q/(2\pi z^2)$ along the line of symmetry [19], p. 140. Thus equating viscous forcing by the *unperturbed* flow field with surface tension leads to $3\eta Q/(2\pi h^{*2}) \sim \gamma$ for the distance h^* where the singularity is expected to occur. This is consistent with the data presented in Fig. 4, if we assume that the point sink is placed a small distance $h_a = 0.29a$ *inside* the hole of diameter $a = 1$ mm. Thus the singularity

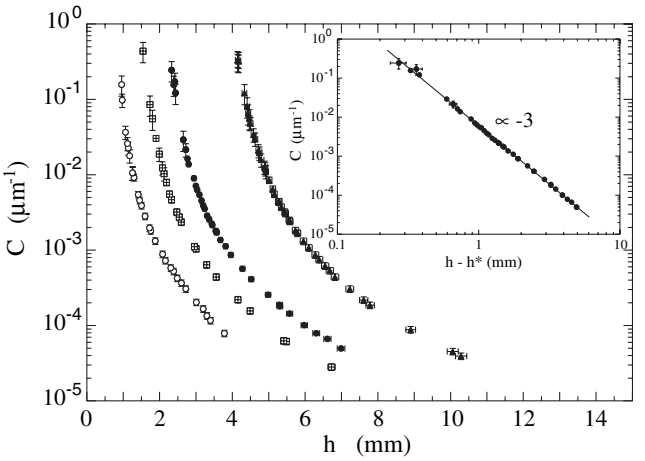

FIG. 3. Tip curvature C as a function of h for silicone oil ($\eta = 30$ Pa s, $\gamma = 2.13 \times 1.0 \times 10^{-2}$ Nm^{-1}), $a = 1$ mm and $Q = 1.7 \times 10^{-3}$ ml s^{-1} (○), 5.1×10^{-3}ml s^{-1} (⊞), 10^{-2}ml s^{-1} (●); and for $a = 3$ mm and $Q = 3.9 \times 10^{-2}$ml s^{-1} (▲). Errors in the curvature represent typical deviations between Gaussian and parabolic fits, whereas errors of 1.5% in h come from the finite range of focus. Inset: log-log plot of C versus $h - h^*$ for $Q = 10^{-2}$ml s^{-1}.

is characterized by the *local* capillary number

$$\mathrm{Ca}\,(h) = \frac{3Q\eta}{2\pi(h + h_a)^2\gamma} \tag{1}$$

reaching a critical value

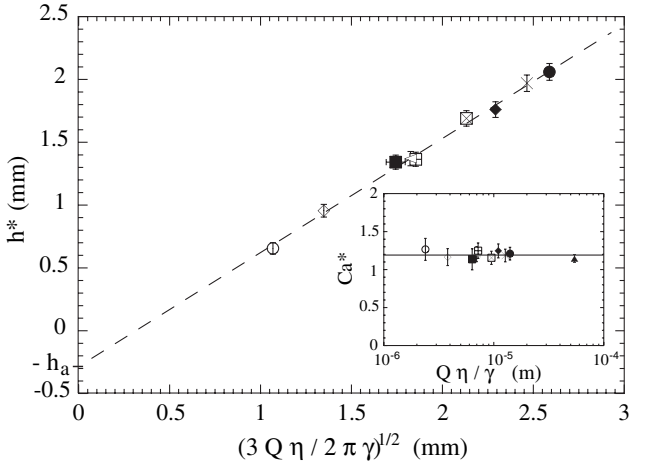

FIG. 4. Critical $h = h^*$ with $a = 1$ mm for silicone oil ($\eta = 30$ Pa s) and Q/ml s$^{-1} = 1.7 \times 10^{-3}$ (○), 5.1×10^{-3}(⊞), 6.8×10^{-3} (⊞), 9×10^{-3} (×), 10^{-2} (●); silicone oil ($\eta = 60$ Pa s) and Q/ml s$^{-1} = 1.4 \times 10^{-3}$ (◇), 2.5×10^{-3} (◁), 3.9×10^{-3} (◆); castor oil and Q/ml s$^{-1} = 0.23$ (■). Errors in h^* come from the absolute measurement of the orifice position: parameters for castor oil are $\gamma = 3.53 \pm 0.1 \times 10^{-2}$ Nm^{-1}, $\eta = 0.93 \pm 0.01$ Pa s. Inset: capillary number Ca* for all experiments [same symbols, ▲: $a = 3$ mm with silicone oil ($\eta = 30$ Pa s) and Q/ml s$^{-1} = 3.9 \times 10^{-2}$].

$$\mathrm{Ca}\,(h^*) \equiv \mathrm{Ca}^* = 1.2 \pm 0.06. \quad (2)$$

This is confirmed in the inset of Fig. 4 using all our data sets, obtained with two different tube openings $a = 1$ mm and $a = 3$ mm. For the shift we used $h_a = 0.29a$, a form consistent with a transition from a sink to a Poiseuille flow [20].

Utilizing the experimental observation that the *prefactor* of the curvature scales like $\sqrt{Q}$ for a given liquid, we can collapse *all* the curvature data into a single scaling law:

$$C = (1.08 \pm 0.06)\frac{[Q\eta/(\rho g)]^{1/2}}{(h - h^*)^3} = 1.88\,\frac{l_c(h^* + h_a)}{(h - h^*)^3}, \quad (3)$$

where $l_c = \sqrt{\gamma/(\rho g)}$ is the capillary length. Figure 5 shows the master curve corresponding to (3) for all our experiments, covering 4 orders of magnitude in the curvature. As expected, (3) says that the curvature increases with flow rate, while gravity tends to flatten the interface. Surface tension is contained implicitly through the dependence on h^*, given by (2). It is instructive to also split the right-hand side of (3) into dependencies on the ''internal'' variable h and on the ''external'' capillary length l_c, which is required on dimensional grounds. Silicone oil and castor oil have capillary lengths l_c of 1.49 and 1.94 mm, respectively, so we have good experimental evidence that it is indeed l_c that sets the external length scale in (3), rather than the size of the cell.

We now turn to the interface shape for $h < h^*$, for which the tip is singular, and the profile meets the tip with a finite slope $R'(h)$. As the hole is approached, the slope becomes small, suggesting the use of slender-body theory [21–23]. In this limit, the perturbation of the axial flow by the interface is small, so it can be represented as a line distribution of 2D sources [23]. For the slope of the interface at the tip we thus find

$$R'(h) = 1/[2\mathrm{Ca}(h)], \quad (4)$$

where Ca is given by (1). Qualitatively, (4) results from the ratio of the unperturbed flow speed in the z direction and the capillary speed γ/η contracting the profile in the r direction, while gravity is irrelevant near the tip.

The slope R' was determined experimentally by fitting $R(z)$ with a second order polynomial in $|z - h|$ and extrapolating to the tip. The result, shown in Fig. 6, is in excellent agreement with the predicted slope, in particular, for small opening angles, as expected. The prefactor is 0.43 ± 0.1, only slightly smaller than the predicted value of 0.5. To estimate the local capillary number, we included the correction h_a deduced from h^*. This we believe to be the first quantitative test of this classical slender-body theory, previous comparisons being only qualitative [24]. The shaded region of Fig. 6 corresponds to *smooth* profiles below the critical capillary number, where we took the minimum value of $R'(z)$ as the slope. Its value merges smoothly into the singular region. At the transition $\mathrm{Ca} = \mathrm{Ca}^*$, the interface slope assumed a universal value of $R'(h^*) = 0.47 \pm 0.06$ for all our experiments.

Discussion.—Our study was motivated by the aforementioned viscous withdrawal experiment [8,15], which found the tip to disappear at a typical size of 200 μm, independent of the viscosity ratio λ between the two liquids. This differs markedly from both theory [23] and experiment [24] with drops of small viscosity in strong flows, which develop tips which are locally similar, but which remain stable well into the singular regime. We thus expected the disappearance of the tip [8] to be related to the far-field boundary condition, which is a flat interface for viscous withdrawal, but a curved interface for drops.

However, at the resolution of the present experiment ($\approx$1 μm), no air entrainment was ever observed. In fact,

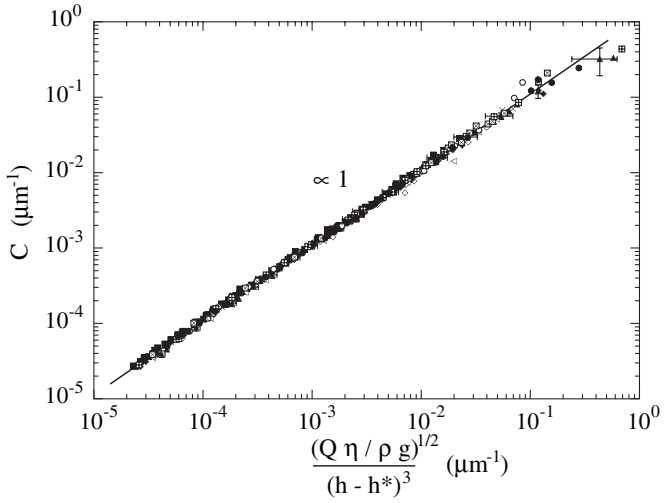

FIG. 5. Master curve, collapsing all data according to (3). Symbols are the same as in Fig. 4. Castor oil data with $C^{-1} \leq 25$ μm are not shown, owing to dust perturbing the tip.

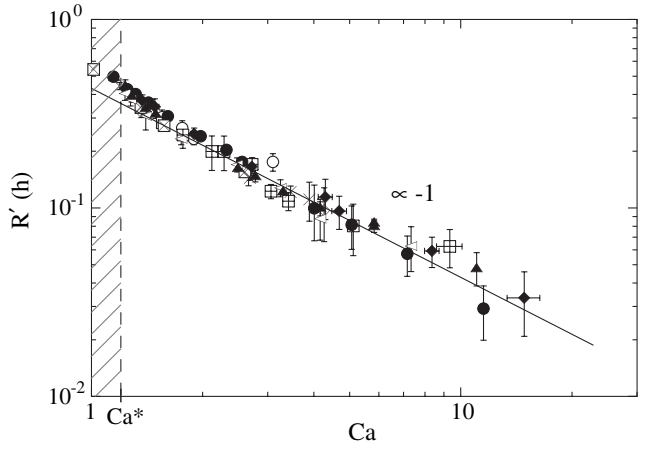

FIG. 6. Slope $R'(h)$ versus Ca for all experiments but the one with castor oil. Same symbols as in Fig. 4. Line: best fit with $R'(h) = (0.43 \pm 0.1)/\mathrm{Ca}$. In the shaded region the slope is defined as the minimum value of $R'(z)$.

air bubbles suspended above the sink hole [25] give results very similar to the ones described here, except that the curvature scaling does not extend to as small values, owing to the bubble curvature. We have considered a number of possible causes for the liquid-liquid and the liquid-air system to behave differently, yet were not able to single out a likely mechanism: (a) In [15] it was proposed that the minimum tip size behaves approximately as $C_{\mathrm{min}}^{-1} \sim 0.1\sqrt{\gamma/(\Delta\rho g)}$, owing to the stabilizing effect of the density difference $\Delta\rho$ between the two liquids. However, this gives a minimum tip size of 150 μm for a liquid-air experiment, in disagreement with our observations. (b) Our viscosity ratios (between $\lambda \equiv \eta_{\mathrm{air}}/\eta_{\mathrm{liquid}} = 3 \times 10^{-7}$ and 2×10^{-5}) are smaller than those of [15]. However, in neither experiment could a significant dependence on λ be detected. (c) Surfactants are known to lead to the ejection of a jet out of the tip of bubbles [26] (''tip streaming''). However, care was taken in [15] to differentiate this transient phenomenon from the reported instability. (d) Finally, it remains to mention the possible effects of compressibility, solubility, and of evaporation into the gas, which distinguish a gas most markedly from a liquid. In fact solubility has, in the two-dimensional analogue of the present problem, been suggested [27] as a mechanism to relieve the pressure that builds up inside a cusp, and which leads to its eventual disappearance [5]. However, one will require a better knowledge of the flow near the tip to estimate the correct pressure balance in the present axisymmetric case. It should also be noted that once a tip size of 1 μm is reached, the mean free path of the air will come into play.

As long as the tip is above the orifice, no air entrainment occurs. However, the indirect evidence of air bubbles appearing at the other end of the tube shows that a spout is formed once the tip enters the orifice. In fact, this setup has been used to create monodisperse streams of bubbles [16]. When subsequently the filling height H is increased again to raise the tip above the orifice, no spout is observed. Rather, a stable tip reappears at $h = 0$, giving no evidence for hysteresis. Thus the experimental protocol suggested in [18] fails to produce a thin spout, a fact that could be related to our far-field conditions being different from those of [18].

A theoretical understanding of the scaling law (3) remains a challenge. Likely, such an understanding will require the description of the entire interface profile. Rescaling the profiles using C^{-1} as a characteristic scale has lead to data collapse only in a very limited region around the tip. Evidently the profiles contain several length scales that need to be included into a proper description.

In conclusion, we have developed a scaling law for the formation of an axisymmetric tip singularity on a liquid-air interface. Singular tips are well described by slender-body theory. Our analysis raises the possibility of using hydrodynamics to produce structures of virtually unlimited smallness.

We are grateful to R. Deegan for his help in designing the experiment and his continued support, and to I. Cohen, R. Kerswell, and É. Lorenceau for very helpful discussions.

[1] J. Eggers, Phys. Rev. Lett. **71**, 3458 (1993).
[2] A. Rothert, R. Richter, and I. Rehberg, Phys. Rev. Lett. **87**, 084501 (2001).
[3] J. Eggers, J. Lister, and H. Stone, J. Fluid Mech. **401**, 293 (1999).
[4] L. Landau and E. Lifshitz, *Fluid Mechanics* (Pergamon, Oxford, 1984).
[5] J. Eggers, Phys. Rev. Lett. **86**, 4290 (2001).
[6] E. Lorenceau, F. Restagno, and D. Quéré, Phys. Rev. Lett. **90**, 184501 (2003).
[7] G. Taylor, Proc. R. Soc. A **146**, 501 (1934).
[8] I. Cohen and S. R. Nagel, Phys. Rev. Lett. **88**, 074501 (2002).
[9] S. Chaieb, physics/0404088.
[10] J. Eggers, in *A Perspective Look at Nonlinear Media in Physics, Chemistry, and Biology*, edited by J. Parisi, S. C. Mueller, and W. Zimmermann (Springer, Berlin, 1998), p. 305.
[11] L. Kadanoff, Phys. Today **50**, No. 9, 11 (1997).
[12] J.-T. Jeong and H. Moffatt, J. Fluid Mech. **241**, 1 (1992).
[13] H. Stone, Annu. Rev. Fluid Mech. **26**, 65 (1994).
[14] A. Gañán-Calvo, Phys. Rev. Lett. **80**, 285 (1998).
[15] I. Cohen, Phys. Rev. E **70**, 026302 (2004).
[16] A. Gañán-Calvo and J. Gordillo, Phys. Rev. Lett. **87**, 274501 (2001).
[17] H. Stone, A. Stroock, and A. Ajdari, Annu. Rev. Fluid Mech. **36**, 381 (2004).
[18] W. Zhang, Phys. Rev. Lett. **93**, 184502 (2004).
[19] J. Happel and H. Brenner, *Low Reynolds Number Hydrodynamics* (Prentice-Hall, Englewood Cliffs, NJ, 1965).
[20] E. Hinch (private communication).
[21] G. Taylor, in *Proceedings of the 11th International Congress of Applied Mathematics*, edited by G. Batchelor (Springer, Heidelberg, 1966).
[22] J. Buckmaster, J. Fluid Mech. **55**, 385 (1972).
[23] A. Acrivos and T. Lo, J. Fluid Mech. **86**, 641 (1978).
[24] B. Bentley and L. Leal, J. Fluid Mech. **167**, 219 (1986).
[25] S. Courrech du Pont and J. Eggers (unpublished).
[26] R. de Bruijn, Chem. Eng. Sci. **48**, 277 (1993).
[27] D. Jacqmin, J. Fluid Mech. **455**, 347 (2002).